

Measurement and Prediction of Aeolian Sediment Transport at Jandía Isthmus (Fuerteventura, Canary Islands)

J. Alcántara-Carrió[†] and I. Alonso[‡]

[†] Dpto. de Geociencias
Marinas y O. T.
Universidad de Vigo
36200 Vigo (Pontevedra),
Spain
carrio@uvigo.es

[‡] Dpto. de Física
Universidad de Las Palmas
de Gran Canaria
35080 Las Palmas, Spain
ignacio.alonso@fisica.ulpgc.es

ABSTRACT

ALCÁNTARA-CARRIÓ, J. and ALONSO, I., 2002. Measurement and prediction of aeolian sediment transport at Jandía Isthmus (Fuerteventura, Canary Islands). *Journal of Coastal Research*, 18(2), 300–315. West Palm Beach (Florida), ISSN 0749-0208.

Predictive models of aeolian sediment transport are calibrated and validated with empirical measurements in the Jandía Isthmus (Canary islands), which consists of a wide diversity of aeolian environments, from dunes to sand sheets and serif areas. Empirical aeolian sediment transport rates measured by vertical sand traps simultaneously with wind velocity profiles permit validation of such models, as well as selection of the best performing equation. The model of ZINGG (1953) for horizontal or nearly-horizontal surfaces and the model of HARDISTY and WHITEHOUSE (1988) applicable to dipping surfaces have shown the best agreement with measurements. In this paper, a new equation is defined and applied to predict the monthly and annual aeolian sand transport at the site.

Sediment flux was found to be mainly to the South or South-Southeast, caused by the dominant northerly trade winds as well as the local topography. Wadis channel the wind and associated transport, but a high transport also occurs to the southwest along the windward coast. Therefore, supply of sediments to both coastal sides has been quantified and the pattern of flux described. Sand blown from Jandía Isthmus constitutes a significant source of materials for both the leeward and windward beaches.

ADDITIONAL INDEX WORDS: *Wind profiles, grain-size, density, sand traps, calibration, Canary Islands.*



INTRODUCTION

It is a well-known fact that the relationship between wind energy and sediment properties determines aeolian sediment transport mechanisms. Three basic mechanisms are suspension, saltation and creep, although hybrid mechanisms have also been described (TSOAR and PYE, 1987). Several models permit calculation of aeolian sand transport as a function of wind parameters (*shear stress, threshold shear stress, and threshold velocity*), sediment properties (size and density) and surface *roughness*.

The formulae of BAGNOLD (1941) and KAWAMURA (1951) are the most accepted because they have a theoretical background and have been verified by numerous experiments, while the models of CHEPIL (1945), ZINGG (1953), WILLIAMS (1964) and HSU (1973, 1977) have been considered as empirical modifications (HORIKAWA *et al.*, 1986).

However, all these above models have been developed for idealised surfaces: horizontal, dry, unobstructed and unvegetated surfaces (SHERMAN and HOTTA, 1990), conditions that are seldom found in true coastal aeolian environments. These environments are characterised by the influence of various environmental factors, such as vegetation (LANCASTER and

BAAS, 1998), humidity content (LOGIE, 1982, SEELIGER *et al.*, 2000), slope (HARDISTY and WHITEHOUSE, 1988) and human pressure (NORDSTROM, 1994). Therefore, the application of the aforementioned aeolian transport models in coastal areas must be calibrated with measurements of environmental factors and aeolian sand transport rates.

Uncertainty in long-term predictions is obviously higher than in short-term predictions, but long-term predictions are necessary to analyse evolution of sedimentary environments. Measurement of wind-speed profiles over reversing dunes show the feedback relationship between flow and form as morphology tends to an equilibrium shape with respect to the prevailing wind in each season (BURKINSHAW *et al.*, 1993). This result suggests that, although *focal points* vary (MC-EWAN and WILLETTS, 1993), an average value during saltation can be obtained for each season and surface, which is useful to predict the annual aeolian sand transport rate.

Aeolian sediment transport studies are hence necessary to understand the sedimentary dynamics of many coastal areas. Erosion or accretion on beaches is generally reflected in the associated aeolian environments, which in turn act as a source or sink of sediments. Several marine and aeolian processes are involved in this balance of materials, each one with their own direction, intensity and temporal variability (SHORT

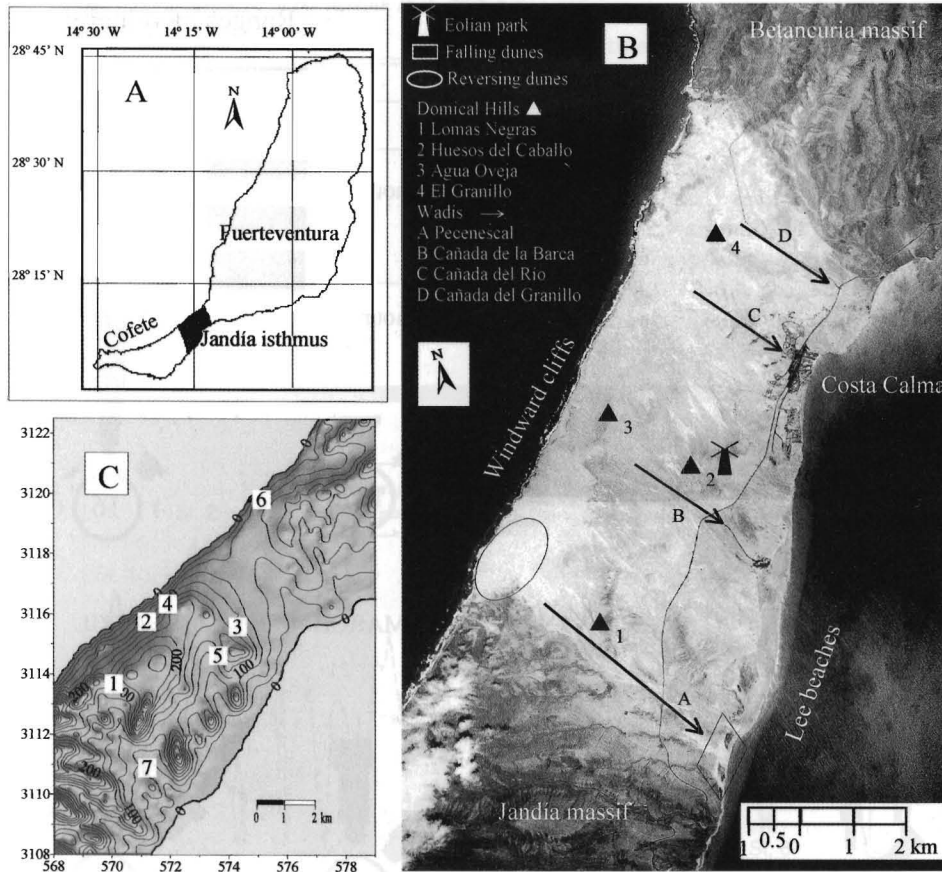


Figure 1. Location of the study area. A) Fuerteventura Island. B) Aerial photography of 1992. C) Topographic map and position of the stations in February and August of 1998.

and HESP, 1982). Orientation of coastline is another factor that must be considered (BAUER *et al.*, 1996). It is generally accepted that this interaction works in the following way: small waves produce a net onshore transport to the foreshore, and strong winds remove this material normally to the back-

shore to form aeolian dunes. These dunes supply sediments in both directions, either to adjacent lagoons and coastal plains, or to the beach, depending on wind direction.

By contrast, the architecture of continental arid environments generally consists of bare rock surfaces, pediments,

Table 1. Main equations used to evaluate the aeolian sand transport.

Author	Equation	Footnotes
BAGNOLD (1941)	$q = C(\rho_s/g) \cdot (d/D)^{1/2} \cdot U_*^3$	q: flux of sediments ($\text{kg m}^{-1} \text{s}^{-1}$) C: empirical coefficient related to sorting and mean grain size. $C = 1.5; 1.8 \text{ or } 2.8$ d: mean grain size of sample in mm D: standard mean grain size of 0.25 mm
KAWAMURA (1951)	$q = K \cdot (\rho_s/g) \cdot (U_* + U_{*c})^2 \cdot (U_* - U_{*c})$ $\forall U_* > U_{*c}$	K: empirical coefficient. $1 \leq K \leq 2.78$ U_{*c} : Threshold shear stress
ZINGG (1953)	$q = Z \cdot (\rho_s/g) \cdot (d/D)^{3/4} \cdot U_*^3$	Z: empirical coefficient ($Z = 0.83$)
WILLIAMS (1964)	$q = a' \cdot (\rho_s/g) \cdot U_*^{b'}$	a' and b' : empirical coefficients $a' = 0.17; b' = 3.42$ for sand
HSU (1973, 1977)	$q = H \cdot \text{Fr}^3 = H \cdot U_*^3 \cdot (g \cdot d)^{-3/2}$	H: empirical variable $H = 10^{-4} \cdot \exp(-0.47 + 4.97 \cdot d)$ Fr: Froude number ($\text{Fr} = U_* \cdot (g \cdot d)^{-1/2}$)
LETTAU and LETTAU (1978)	$q = L (d/D)^{1/2} \cdot (\rho_s/g) \cdot U_*^2 \cdot (U_* - U_{*c})$ $\forall U_* > U_{*c}$	L: empirical coefficient ($L = 4.2$)

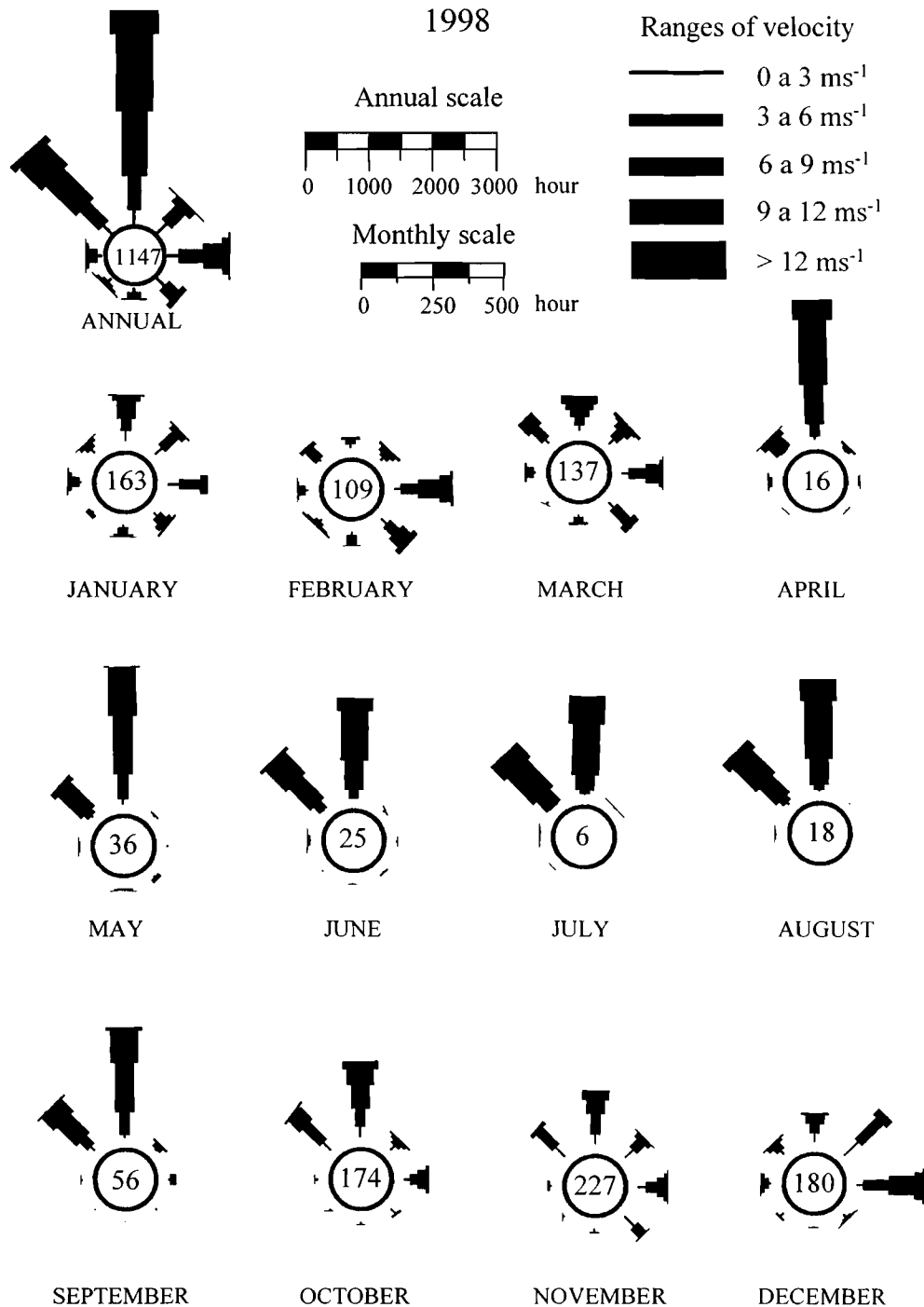


Figure 2. Monthly and annual wind roses for Jandía Isthmus from data collected at the Aeolian Park of Cañada del Río.

alluvial fans, intermittent streams, dunes, sabkhas and playas, where the source area of sediments is from their own continental environments (FRIEDMAN and SANDERS, 1978).

The selected study area is a coastal zone with a complex geomorphology resulting from a geological history that has undergone several climatic changes (CRIADO, 1991; MECO,

1993). Outcrops of volcanic materials, pediments, dry wadis, sand sheets, and different kinds of dunes and beaches are present. ALCÁNTARA-CARRIÓ *et al.* (2000a, 2000b) have shown that fragments of marine shells, algae, and foraminifera primarily comprise the surface sediments and that currently the windward coast does not supply materials to the Jandía Isth-

Table 2. Number of hours during 1998 for each velocity range and direction of the wind at Jandía Isthmus. Data measured at the Aeolian Park of Cañada del Río.

1998 Velocity Ranges	Wind Direction							
	N	NE	E	SE	S	SW	W	NW
0–3 ms ⁻¹	218	211	182	162	64	63	71	176
3–6 ms ⁻¹	542	308	387	214	105	41	136	420
6–9 ms ⁻¹	1045	135	294	100	30	33	49	670
9–12 ms ⁻¹	1240	0	101	0	2	13	10	476
>12 ms ⁻¹	385	0	19	0	0	7	0	128

mus. For this reason the study area can be considered as an intermediate case between the standard behaviour of coastal and continental arid environments mentioned above.

The method of study of aeolian environments is dependent on the spatial scale being considered. Aeolian architecture is composed of micro-, meso-, macro- and mega-scale features related to textural properties, aeolian processes, bed form dynamics and global evolution, respectively (CLEMMENSEN, 1993). The temporal variability of aeolian dynamics is related to the variability of wind, sediments and environmental factors. LARSON and KRAUS (1995) have defined the temporal ranges for the micro-scale (second-minute), meso-scale (hour-day), macro-

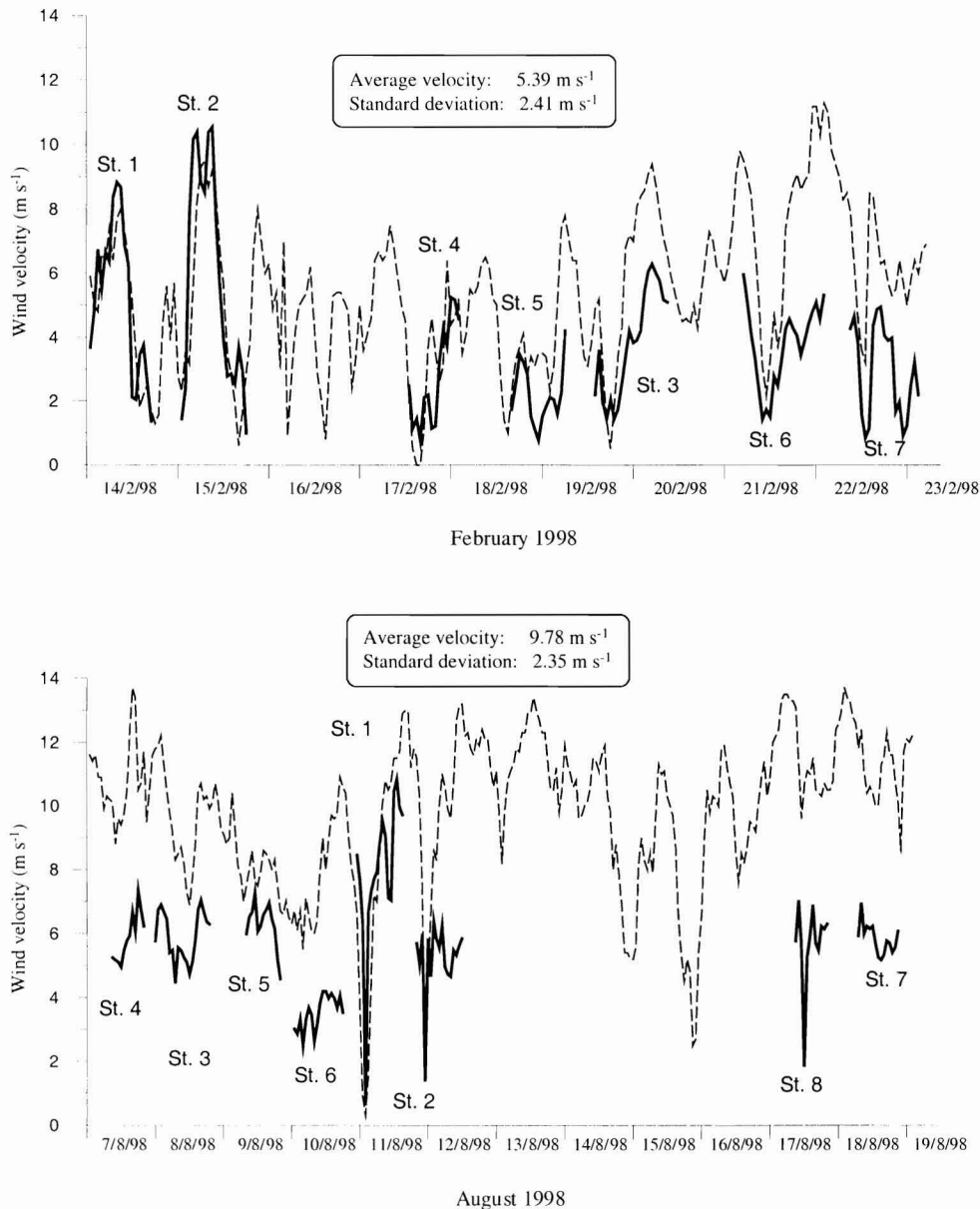


Figure 3. Wind data recorded by the sensor of the anemometer tower placed at 1-m high in each station (continuous line) and by the meteorological station of the Aeolian Park of Cañada del Río (dashed line). Statistical values correspond to wind data of the aeolian park during each fieldwork period.

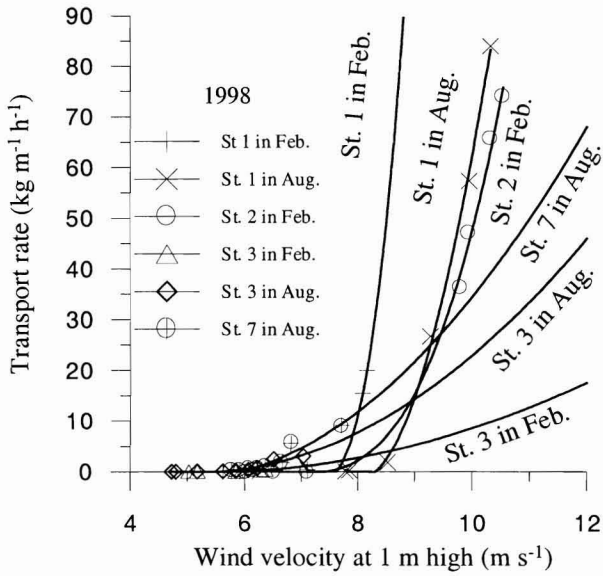


Figure 4. Graphic relation and polynomial fits between wind velocity measured at 1-m high and the transport rates obtained by sand traps.

scale (month-year) and mega-scale (10^2 – 10^3 years), which are compatible with the ranges of the spatial scale. The goal of this work is the prediction of aeolian sediment transport across the Jandía Isthmus at an annual time scale. This study is therefore concerned with the spatial and temporal macro-scale level, but is based on data taken at the meso-scale. Physical models based on wind and sediment parameters consider meso-scale aeolian processes. Potential transport rates predicted from these models are calibrated with empirical sand transport rates measured in different seasons and locations. Finally, annual sand transport rates are obtained with the calibrated equations and annual wind data.

STUDY AREA

Fuerteventura is the oldest island of the Canary Archipelago. Its basal materials consist of Cretaceous turbidites overlain by interbedded Albian-Oligocene sediments and submarine volcanic materials, that are intruded by a dense dyke network and alkaline plutonic rocks (LE BAS *et al.*, 1986). Three stages have been described in the formation of intraplate oceanic volcanic islands: i) Shield-stage, initial volcanic period that built more than 90% of total volume, ii) Erosional gap, iii) Post-erosional volcanism (MCDONALD *et al.*, 1970). Fuerteventura, Lanzarote and Gran Canaria islands are now in the last stage, while the La Gomera island is currently undergoing an erosional gap and the Tenerife, La Palma and El Hierro islands are still in the shield-stage (CARRACEDO *et al.*, 1998). The geomorphology of the Canary Islands is not only the result of these volcanic processes, but also other geological agents that have modified their surface, producing a diverse relief. Rainy periods have formed valleys, glacis, and wadis (CRIADO, 1987, 1991), while marine action has produced cliffs, beachrocks, beaches and dune deposits (MECO, 1993).

Table 3. Threshold shear stress and maximum shear stress for each station whose focal point is known.

	February 1998			August 1998		
	Station 1	Station 2	Station 3	Station 1	Station 3	Station 7
Theoretical U_{*c} (m/s)	0.27	0.30	0.23	0.32	0.26	0.29
Empirical U_{*c} (m/s)	0.23	0.07	0.25	0.23	0.13	0.40
Maximum U_* (m/s)	0.44	0.24	0.29	0.57	0.23	0.57

The Jandía massif (17–14.2 Ky, COELLO *et al.*, 1992) is the southernmost of the three shield volcanoes of Fuerteventura. The subaerial surface connecting it with the rest of the island is the Jandía Isthmus, a surface with an extension of 54.2 km² (4.2–6.5 km width per 10.5 km length, approximately). The isthmus has a smooth low relief, with a mean elevation of 130 m and a maximum elevation of 322 m (Lomas Negras). Other relevant hills are Risco del Paso (253 m), and Agua Oveja (213 m). These low dome hills consist of volcanic materials, that are covered in many cases with carbonate crusts. Several short wadis cross the area in a NNW-SSE direction, the most important ones sloping to the leeward coast (Cañada del Granillo, Cañada del Río, Cañada de la Barca, and Barranco de Pecenesal). The main feature of the isthmus is the great diversity of aeolian environments including serir, sand sheets and dune deposits, which together represent the largest aeolian surface of the Canary Islands (Figure 1). The isthmus exhibits a complex geomorphology and sedimentary dynamics; aeolian processes currently dominate it.

The windward coast of the isthmus is at present an active cliff with a basaltic base, a Messinian terrace (+3 m) and consolidated aeolian deposits that reach up to 30-m thickness in some areas. Cofete Beach is located south of Jandía Isthmus along the windward coast. Geomorphologic, textural, and compositional data have shown that the marine environments, both windward and leeward, do not supply sediments to the aeolian deposits (ALCÁNTARA-CARRIÓ *et al.*, 2000a, 2000b). By contrast, a great amount of sediment is blown from the isthmus towards the leeward coast, which contains an inactive cliff with falling dunes and wide beaches. Therefore, the quantification of the aeolian sediment transport is a fundamental requirement for the characterisation of the sedimentary dynamics of these beaches.

Tourism has seen a large increase in the area during the last decades with resorts and roads built near the leeward beaches. These actions modify the local wind flow, distribution of the vegetation, sediment surface properties and can even act as impermeable walls to aeolian sand transport. Accordingly, a decrease of aeolian sediment supplied to the leeward beaches could increase beach erosion which would threaten, if not remove, the basic tourism resource (HÖLLERMANN, 1990; MONTESDEOCA *et al.*, 2000).

METHODOLOGY

Wind Measurements

During 1998 hourly wind velocity and direction data were measured at the Aeolian Park of Cañada del Río (20 m

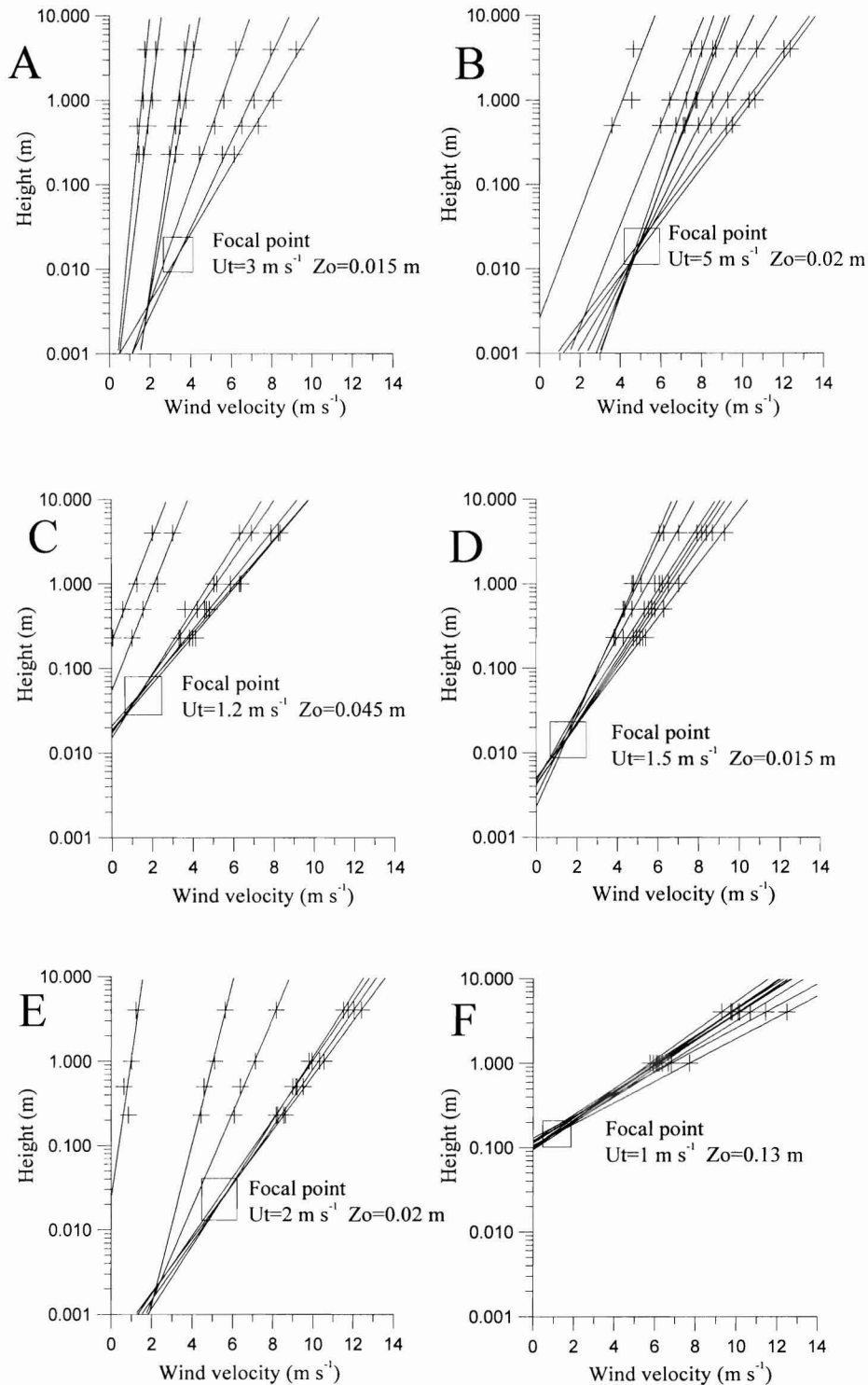


Figure 5. Use of wind profiles to identify the *focal point* and related wind parameters in the stations with effective transport rates. A) Station 1 in February. B) Station 1 in August. C) Station 3 in February. D) Station 3 in August. E) Station 2 in February. F) Station 7 in August.

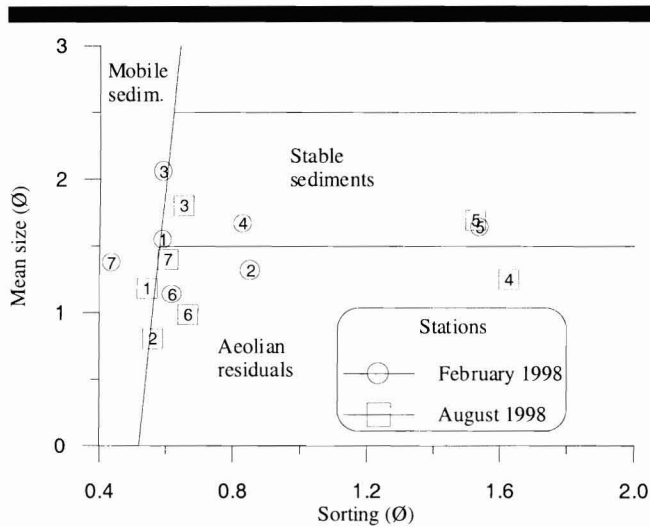


Figure 6. Classification of the aeolian surface deposits corresponding to each station using the mean size against sorting diagram of GLASER (1984).

height). Unfortunately, only 23 hourly readings per day were recorded and technical failures caused several gaps, yielding a total of 723 hours without data (8.2%). Annual and monthly wind roses were plotted for this period using eight principal wind directions (N, NE, E, SE, S, SW, W, and NW) and five velocity ranges (0–3, 3–6, 6–9, 9–12, and >12 m/s).

More detailed studies of the wind blowing over the different aeolian environments of the isthmus were carried out in two surveys, during February and August 1998. Seven stations were chosen during each survey (Figure 1). Wind velocity profiles were measured by an Aanderaa anemometer tower with cup anemometers at 0.23, 0.5, 1, and 4 m high and a wind vane at 2 m high. This anemometer tower was placed at each station for 24 hours, with a sampling frequency of 5 minutes for all sensors.

Correlation between the wind data recorded at 1-m height and the Cañada del Río (20-m height) meteorological station permitted the prediction of the hourly wind velocity at 1 m during the whole year at each station. Horizontal velocity variations were derived by comparison of the predicted annual wind data at the stations.

Sediment Transport Measurements

A set of 4 sand traps was placed facing to N, S, E, at each station near to the anemometer tower. Vertical sand traps based on LEATHERMAN (1978) design were deployed, although some modifications were made (ALCÁNTARA-CARRIÓ and ALONSO, 2000). The most significant of these was an apron placed around the trap, with its periphery buried into the sand to avoid scouring around the trap mouth, following the idea proposed by ILLENBERGER and RUST (1986). A sampling period of 5 minutes per hour was also used for the traps to compare measurements with simultaneous wind data. Net transport rates were calculated by weighing trapped sand within each trap during the same interval and by directional addition of the data.

Physical Parameters of the Models

Wind velocity profiles allow the calculation of a focal point, whose height is a measure of the roughness length (z_0) while the associated wind speed is the threshold velocity (U_t) (BAGNOLD, 1941). In this work the positions of the focal point were only calculated at the stations where sand transport rates were higher than a threshold rate of 0.01 kgm⁻¹h⁻¹. In order to predict the annual sand transport when it was only possible to determine the focal point for one study period, it was considered as uniform at this station during the whole year. Shear stress (U_{*c}) for each velocity profile was calculated from the focal point and wind velocity data at a height of 1 m using the BAGNOLD (1941) modified expression of the law of the wall (I). Threshold shear stress (U_{*t}) for each station was calculated by two methods: i) from empirical data, being the shear stress measured when the aeolian sand transport rates were higher than the chosen threshold, and ii) using the theoretical expression (II) of BAGNOLD (1941).

$$U_z = (U_{*c}/k) \cdot \ln(z/z') + U_t \tag{I}$$

$$U_{*t} = A((\rho_s - \rho_a/\rho_a) \cdot g \cdot d)^{1/2} \tag{II}$$

where U_z is the wind velocity at a height of z m, k is the constant of VON KARMAN (1934), equal to 0.4 (FRENZEN and VOGEL, 1995), ρ_s is the sediment density, ρ_a is the air density, g is the acceleration due to gravity, d is the mean grain size, and A is the square root of the Shields Function (e.g. MILLER et al., 1977) equal to 0.1 (BAGNOLD, 1941; SARRE, 1987) when

Table 4. Sedimentary and environmental parameters determined for the surface deposits at each station in February 1998.

Station	Grain Size Parameters (Phi units)				Density (kgm ⁻³)	Carbonate Content (%)	Slope (°)	Bushy Vegetation		Herbaceous Vegetation	
	M_i	σ_i	Sk_i	K_G				High (m)	Cover (%)	High (m)	Cover (%)
1	1.55	0.59	0.18	1.28	2,713.2	98.22	0	0	0	0	0
2	1.32	0.85	0.00	0.99	2,732.1	96.69	-7	0	0	0	0
3	2.06	0.59	0.26	1.26	2,722.2	96.68	-3	0.28	4.92	0.08	0.42
4	1.67	0.83	-0.10	1.22	2,721.4	96.80	-10	0.17	6.16	0.02	9.20
5	1.64	1.54	-0.27	1.76	2,711.2	98.56	+6	0.30	2.64	0.01	14.12
6	1.14	0.62	0.36	1.29	2,741.7	93.30	-6	0.22	4.76	0.02	8.00
7	1.37	0.44	0.04	1.06	2,739.4	93.70	+3	0.44	11.28	0.03	4.80

Table 5. Sedimentary and environmental parameters determined for the surface deposits at each station in August 1998.

Station	Grain Size Parameters (Phi units)				Density (kgm ⁻³)	Carbonate Content (%)	Slope (°)	Bushy Vegetation		Herbaceous Vegetation	
	M _i	σ _i	Sk _i	K _i				High (m)	Cover (%)	High (m)	Cover (%)
1	1.18	0.54	0.63	1.41	3,785.9	94.76	0	0	0	0	0
2	0.81	0.56	0.28	1.56	2,787.3	85.42	-7	0	0	0	0
3	1.80	0.65	0.01	1.00	3,752.5	92.07	-3	0.23	4.20	0	0
4	1.25	1.63	-0.36	1.84	2,754.5	90.18	-10	0.15	4.40	0.02	2.01
5	1.70	1.52	-0.23	1.83	2,760.6	90.19	+6	0.25	1.21	0.02	2.90
6	0.99	0.67	0.30	1.26	2,834.4	83.88	-6	0.30	3.51	0	0
7	1.40	0.61	0.23	1.28	2,722.3	87.84	+3	0.48	9.60	0	0

the Reynolds number is higher than 3.5 (NICKLING and EC-CLESTONE, 1981).

In addition to wind data, a surface sediment sample was taken at each station and study period. Samples were dry sieved at 0.5 φ intervals and graphic parameters were calculated from accumulated frequency distributions (FOLK and WARD, 1957). A Response diagram of mean size against sorting values was used to classify the surface sediments as mobile, stable or residual (BESLER, 1983). However, the graphic limits of GLASER (1984) were chosen instead of those of BESLER (1983) according to the work of HÖLLERMANN (1990).

The density of the sediments was calculated by weighing in a precision balance one 25 ml flask in four stages: empty (P1), with distilled water (P2), with sediments (P3), and with both distilled water and sediments (P4). Density was calculated as:

$$\text{Density} = P3 - P1 / ((P2 - P1) - (P4 - P3)) \quad (\text{III})$$

Each sample was analysed three times and the average value was considered to be the correct density.

Finally, the main environmental factors affecting the aeolian processes were measured for a 10m × 10m area at each station and study period. Vegetation average height and cover percentage were calculated separately for shrub and grass. Topographic slope was measured with a clinometer.

Prediction and Calibration of Aeolian Sand Transport

The predicted hourly wind data, *shear stress*, mean size (M_i), and density of the sediments were used to apply various theoretical models of aeolian sand transport (Table 1). These physical models do not consider environmental factors and there is currently no model that takes into account the combined influence of various environmental factors, such as vegetation cover and height, slope, etc. Influence of local vegetation was not patterned because models are only defined for grass (LANCASTER and BAAS, 1998). Nevertheless, influence of slope was considered using the model of HARDISTY and WHITEHOUSE (1988) for station 2, located on a sloping surface:

$$\begin{aligned} q &= A \cdot K \cdot (U_*^2 - B^2 \cdot U_*^2) \cdot U_* \\ K &= 10^{-5} / (6.6 \cdot d^{1.23}) \\ A &= |\text{tg } i / (\text{tg } i - \text{tg } b)|^7 \\ B &= |(\text{tg } i - \text{tg } b) \cdot \cos b / \text{tg } i|^{1/2} \end{aligned} \quad (\text{IV})$$

where *i* is the threshold slope of the surface, equal to 32° and

b is the real surface slope. Moreover, according to these authors, an alternative expression for the "A" coefficient after BAGNOLD (1956) was also tested:

$$A = (\text{tg } i / \cos b) \cdot (\text{tg } i - \text{tg } b)^{-1} \quad (\text{V})$$

In order to calibrate the accuracy of these models, polynomial curves were fitted to empirical rates. Interpolated rates were then compared with the theoretical rates by a linear fit ($q_{\text{empirical polynomial}} = a \cdot q_{\text{theoretical}}$).

Finally, annual aeolian sand transport rates for each station were predicted. Results were plotted in sand roses for each month and for the whole year, and the transport parameters were calculated after FRYBERGER and DEAN (1979): *Resultant Drift Potential* (RDP), *Resultant Drift Direction* (RDD), *Drift Potential* (DP). RDD is given in the clockwise direction from the N. Ranges of values of the RDP/DP ratio were used to identify unimodal (0.8 ≤ RDP/DP), bimodal (0.3 ≤ RDP/DP < 0.8) or complex (0 ≤ RDP/DP < 0.3) sand transport regimes.

RESULTS AND DISCUSSION

Wind Behaviour

Annual wind roses obtained from hourly data of 1998 shows a clear prevalence of N and NW wind directions for all selected ranges, although the E component is also important (Figure 2 and Table 2). Nevertheless, monthly wind roses clearly show two seasonal periods, in agreement with previous studies of wind behaviour in the study area (ALCÁNTARA-CARRIÓ *et al.*, 1996). This pattern is confirmed by the analysis of hourly wind data measured at the Aeolian Park of Cañada del Río during 1995–1997 (ALCÁNTARA-CARRIÓ, 1999). The N-NW direction occurs during late spring and summer, *i.e.* April to September, which have stronger winds, fewer calm hours and a more uniform wind direction, while the rest of the year has winds that are much more variable in both direction and intensity and most of the calm hours. Another interesting result is that the N-NW direction is identified for the trade winds in the area, instead of the N-NE direction which is characteristic for the Canary Islands. Wind data recorded at the Fuerteventura airport (in the northeastern coast of the island) show prevailing NE winds (CRIADO, 1987). The local westerly component at the study area is due to influence of local topography. In fact, the airport is fully exposed to the trade winds, while the isthmus is placed between two masifs, Betancuria to the NE and Jandía to the SW. Wind is

funnelled between the massifs with a resulting change in direction across the isthmus. This further strengthens the fact that local wind data are essential for any aeolian sediment transport study.

Vertical wind profiles show a logarithmic distribution, as expected (BAGNOLD, 1941; HSU, 1973). Wind velocity data measured at a height of 1 m at each station are in agreement with hourly data recorded at the aeolian park (Figure 3), with R-squared coefficients higher than 0.85 in all cases. Consequently, it is possible to calculate the 1998 hourly wind intensity at any station.

Equation coefficients for stations 1, 3 and 7 are very similar in both seasons, however, there are marked seasonal differences at stations 2, 4 and 6. This different behaviour probably is caused by the local topography at each station, which can significantly reduce strong winds taking place during the summer season. Consequently, the extrapolation of wind velocity to the whole year is carried out in two periods. The coefficients obtained for February 1998 are considered adequate for the period lasting from October to April, and the coefficient for August 1998 for the wind data recorded between May and September. Wind direction during the recording intervals shows small ranges of values, and therefore it is not possible to predict the hourly wind direction for the whole year. Consequently, wind direction for all stations is considered to be similar to Cañada del Río measurements.

Empirical Sand Transport Rates

Transport rates exceeded the chosen threshold ($0.01 \text{ kgm}^{-1}\text{h}^{-1}$) only at stations 1, 2, 3 and 7 which are the ones used to predict annual sand transport. Net empirical rates are very different among them, but they have a clear relation to the 1-m high wind velocity (Figure 4). Polynomial fits indicate that sand transport rates are related with the third power of the wind velocity at stations 1 and 2, while stations 3 and 7 show a second power relation. According to these equations, aeolian sediment transport will be higher in the former group for the same wind energy. Furthermore, during the February sampling period there was a reduction in the number of times sand transport rates exceeded the chosen threshold because wind intensity was less strong.

Wind Parameters

BAGNOLD (1941) defined the *focal point* as the spatial point where wind velocity profiles converge during the saltation process. The definition of *focal point* has been conceptually discussed (OWEN, 1964); MCEWAN and WILLETS (1993) state, however, that instead of a point, wind profiles converge in an area or group of points. Furthermore, three important sources of uncertainty in the analysis of velocity profiles have been associated with inaccuracy and imprecision of the measurements, non-fulfilment of conditions for application of velocity profile equations, and mistakes in statistical procedures (BAUER *et al.*, 1992). Therefore, new mathematical models for short-term aeolian sand transport predictions have been defined, but they are not yet in general use. It is, moreover, questionable whether this approach will ever yield universal transport rate formulae (ANDERSON *et al.*, 1991). In conclu-

sion, the von Karman—Prandtl logarithmic velocity profile law and Bagnold's theory continue to be the basis for present day aeolian sediment transport studies. *Focal points* were determined only for the stations with sand transport rates higher than the selected threshold value ($0.01 \text{ kgm}^{-1}\text{h}^{-1}$). Therefore, stations 1, 2, 3 and 7 represent the most useful in predicting annual sand transport at the site. U_1 and z_0 values are derived from the *focal point* for each station (Figure 5), which are different for each case but within the range of values defined by the literature (BAGNOLD, 1941; BRESSOLIER and THOMAS, 1977).

In this study, two converging points are observed in the velocity profile plots: i) the first one where wind velocity increases in the high zone while roughness of the bed decreases the wind velocity near its surface, but there no transport yet; and ii) the *focal point* where a higher increase in wind velocity permits movement of the surface sediments, mainly by saltation. Once the *focal point* is identified, the U_{*c} is calculated for all 1-m high wind velocity data. Table 3 shows the threshold and the maximum values obtained for each station. In the same table it can be observed that empirical and theoretical threshold values (U_{*c}) are very different. The empirical method can only be applied at stations with measured sand transport (1, 2, 3 and 7), and was chosen because it shows the influence of other environmental factors, while the theoretical equation (II) does not consider them.

Sedimentary Parameters

Surface deposits are composed of fine to coarse, well to poorly sorted, negatively to positively skewed, and normal to leptokurtic sands. Density values are similar to calcite, due to the high carbonate content; calcite, aragonite, and magnesian calcite are present based on X-ray diffraction analysis (ALCÁNTARA-CARRIÓ *et al.*, 2000b). In relation to environmental factors, stations are representative of both windward and leeward sides (positive and negative slopes respectively), while the vegetation cover is mainly shrub with grass present during winter at some stations (Tables 4 and 5).

The magnitude of sand transport is dependent not only on wind intensity, but also on the various sediment properties that determine the ability of the wind to entrain surficial material (BAGNOLD, 1941; ALCÁNTARA-CARRIÓ and ALONSO, 2001). A plot of mean size against sorting, using the criteria of GLÄSER (1984), classifies the surface sediments present at each station as mobile, stable or residual (Figure 6). From this diagram, it can be seen that there are important seasonal variations for each station, but in general, sediments at stations 1, 3 and 7 appear to have a higher transport potential, while sediments at the remaining stations have low remobilization potential.

Predicted Short-Term Sand Transport Rates

Sand transport rates predicted by the models of BAGNOLD (1941), KAWAMURA (1951), ZINGG (1953), WILLIAMS (1964), HSU (1973, 1977), and LETTAU and LETTAU (1978) show large discrepancies among themselves and with the empirical rates (Figure 7). Linear fits between model results and the interpolated polynomial curves determined from empirical rates indicate that predictions from the ZINGG (1953) model have

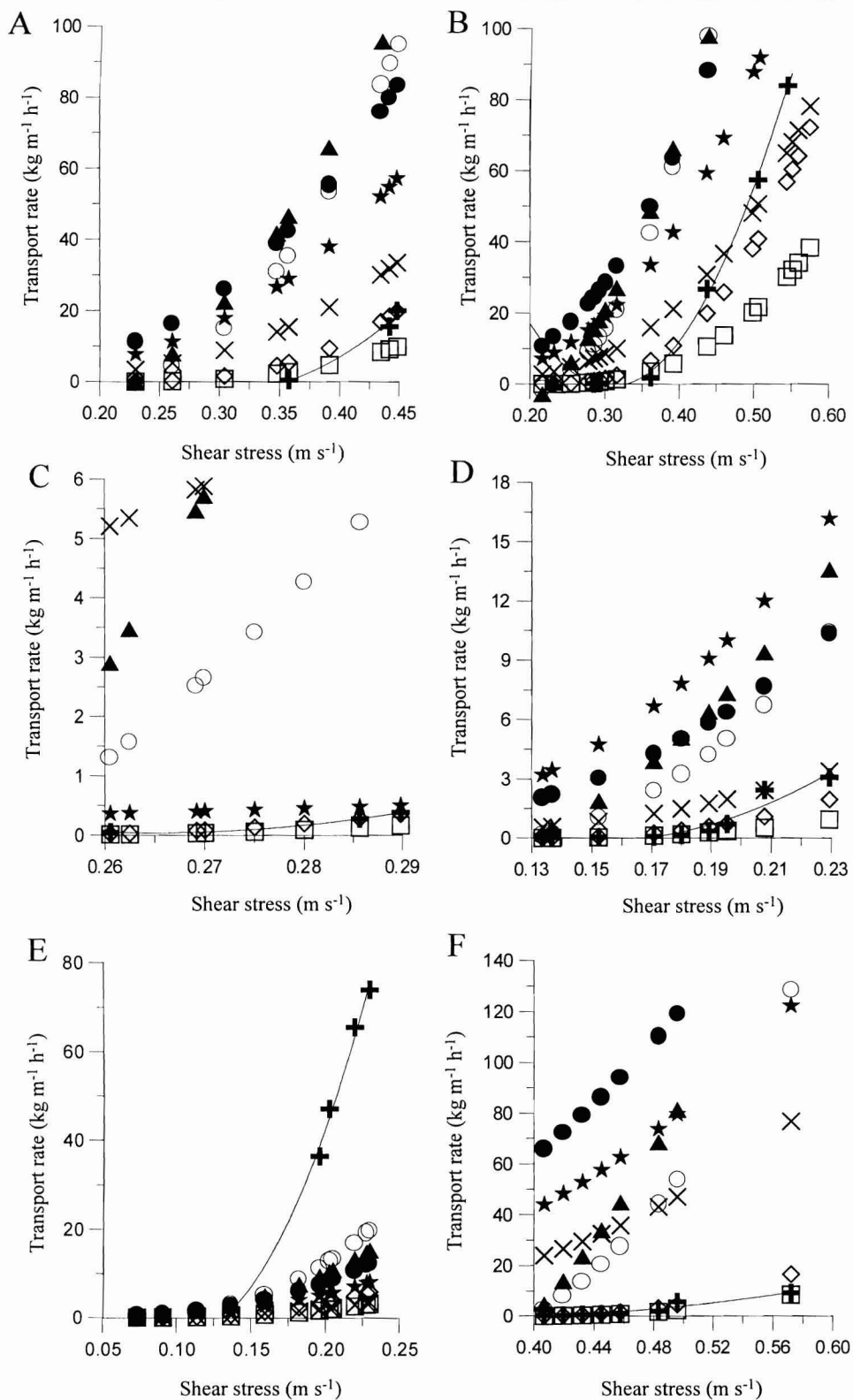


Figure 7. Comparison of the predicted and empirical sand transport rates. A) Station 1 in February. B) Station 1 in August. C) Station 3 in February. D) Station 3 in August. E) Station 2 in February. F) Station 7 in August. Empirical rates: + data, — polynomial fit. Theoretical rates after model of: ● BAGNOLD (1941), ▲ KAWAMURA (1951), □ ZINGG (1953), × WILLIAMS (1964), ★ HSU (1973, 1977), ○ LETTAU and LETTAU (1978), ◇ equation (VI).

Table 6. Equations and R-squared coefficients of the linear fits between the empirical aeolian sand transport rates and the theoretical ones (Y and X respectively).

	Station 1		Station 2	Station 3		Station 7
	February (3 rates)	August (6 rates)	February (5 rates)	February (3 rates)	August (9 rates)	August (8 rates)
BAGNOLD (1941)	Y = 0.19·X R ² = 0.88	Y = 0.42·X R ² = 0.93	Y = 5.84·X R ² = 0.99	Y = 0.01·X R ² = 0.85	Y = 0.19·X R ² = 0.70	Y = 0.03·X R ² = 0.69
KAWAMURA (1951)	Y = 0.15·X R ² = 0.91	Y = 0.37·X R ² = 0.95	Y = 4.68·X R ² = 0.99	Y = 0.03·X R ² = 0.98	Y = 17·X R ² = 0.80	Y = 0.05·X R ² = 0.93
ZINGG (1953)	Y = 1.81·X R ² = 0.96	Y = 2.70·X R ² = 0.99	Y = 24.60·X R ² = 1.00	Y = 2.28·X R ² = 0.99	Y = 3.26·X R ² = 0.92	Y = 1.17·X R ² = 0.92
WILLIAMS (1964)	Y = 0.49·X R ² = 0.90	Y = 1.46·X R ² = 0.98	Y = 21.49·X R ² = 1.00	Y = 0.02·X R ² = 0.70	Y = 0.64·X R ² = 0.74	Y = 0.08·X R ² = 0.73
HSU (1973, 1977)	Y = 0.28·X R ² = 0.88	Y = 0.62·X R ² = 0.92	Y = 8.75·X R ² = 0.99	Y = 0.56·X R ² = 0.85	Y = 0.12·X R ² = 0.70	Y = 0.68·X R ² = 0.68
LETTAU and LETTAU (1978)	Y = 0.18·X R ² = 0.93	Y = 0.34·X R ² = 0.98	Y = 3.70·X R ² = 1.00	Y = 0.06·X R ² = 0.99	Y = 0.25·X R ² = 0.85	Y = 0.45·X R ² = 0.94

the best R-squared coefficients in five of the six stations (Table 6).

Empirical Calibration of Sand Transport Models

Theoretical predictions are especially different from empirical transport rates observed at station 2, which is characterised by a surface without vegetation and with a slope of 7° (Table 4). Results of the HARDISTY and WHITEHOUSE (1988) model show a similar values to the empirical rates, while the models of BAGNOLD (1956) and ZINGG (1953) are markedly dissimilar (Figure 8). Therefore, the model of HARDISTY and WHITEHOUSE (1988) is chosen to predict the annual aeolian sand transport at station 2. A linear fit with this empirical data gives a calibration coefficient of 0.82 which is interpreted as

a roughness length and cohesion differences between a typical dune and this environment. In relation to the model of ZINGG (1953), its empirical coefficient Z has been also calibrated to obtain a better prediction (linear coefficient “a” closer to 1), although the R-squared does not change (Table 7).

A new equation (VI) is proposed which produces a good fit to the empirical sand transport rates (Table 7); it has an expression similar to the equations of BAGNOLD (1941), KAWAMURA (1951) and LETTAU and LETTAU (1978). Physical considerations of BAGNOLD (1941) are valid for this model, where initial sand transport rates are proportional to the third power of shear stress, but some minimum shear stress is necessary to initiate aeolian sediment transport, hence a threshold shear stress is included in the equation.

$$q = F (d/D)^{1/2} \cdot (\rho_a/g) \cdot U_* \cdot (U_* - U_{*t})^2 \tag{VI}$$

where F is a empirically calibrated coefficient, U_{*t} is the empirical threshold shear stress, U_{*} is the empirical shear stress; U_{*} must be higher than U_{*t} to initiate transport.

Equation (VI) has been chosen to predict the annual aeolian sand transport at stations 1, 3 and 7. Similar results are expected from the calibrated equation of ZINGG (1953). Values of Z and F are similar for each station, although the theoretical expressions are different. However, they show a seasonal fluctuation that has been interpreted as the combined influence of the environmental factors, which present both seasonal and spatial variations. Average values for Z of 1.86 and for F of 1.97 were found, excluding station 2. These values are similar to C = 1.8 of BAGNOLD (1941) for medium sand, which is actually the mean grain size of most of the surface sediments at these stations. This comparison seems to indicate that these are reasonable estimates for the average values of Z and F for any station, where the influence of environmental factors is not evaluated. The value of Z = 0.83 obtained in a blow-off wind tunnel by ZINGG (1953) is not in accordance with the empirical results of this study.

Predicted Long-Term Sand Transport Rates

Monthly and annual aeolian sand transport predictions for stations 1, 2, 3 and 7 are shown by plots of annual sand roses (Figure 9) and tables with the related wind regime param-

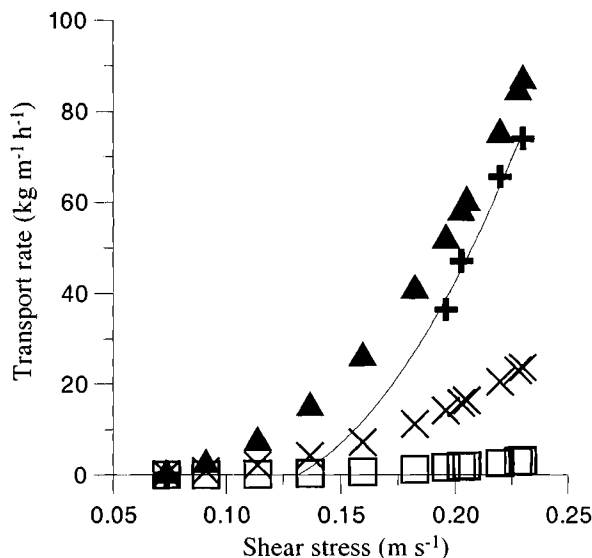


Figure 8. Comparison of the predicted and empirical sand transport rates for station 2. Empirical rates: + data, — polynomial fit. Theoretical rates after model of: ▲ HARDISTY and WHITEHOUSE (1988), × HARDISTY and WHITEHOUSE (1988) but using the equation (V) of BAGNOLD (1956) to calculate the coefficient A, □ ZINGG (1953).

Table 7. Calibrated values of Z and F coefficients, new equations and associated R-squared of the linear fits between the empirical aeolian sand transport rates and the theoretical ones (Y and X respectively).

	Station 1		Station 2	Station 3		Station 7
	February (3 rates)	August (6 rates)	February (5 rates)	February (3 rates)	August (9 rates)	August (8 rates)
ZINGG (1953)	Z = 1.50 Y = 1.00·X R ² = 0.96	Z = 2.24 Y = 1.19·X R ² = 0.99	Z = 20.42 Y = 1.00·X R ² = 1.00	Z = 1.89 Y = 1.00·X R ² = 0.99	Z = 2.71 Y = 1.00·X R ² = 0.92	Z = 0.97 Y = 1.00·X R ² = 0.92
EQUATION (VI)	F = 1.61 Y = 1.00·X R ² = 0.96	F = 2.59 Y = 1.08·X R ² = 0.99	F = 22.96 Y = 1.00·X R ² = 1.00	F = 1.80 Y = 1.04·X R ² = 0.99	F = 2.80 Y = 1.00·X R ² = 0.92	F = 1.08 Y = 1.00·X R ² = 0.92

ters (Table 8 and APPENDIX I). Stations 1 and 7, located in Wadi Pecenescal, have the highest annual rates per unit width (RDP). Stations 1, 7, and 3 have transport directions (RDD) towards S-SSE due to the predominant action of the trade winds. Aeolian transport at station 2 is mainly towards the West which is directly down the slope of this inclined surface. The annual wind regime is unimodal at stations 1 and 7, but bimodal at stations 2 and 3, because of a topographic influence. Aeolian transport at the former stations is

controlled by the orientation of Wadi Pecenescal, while the latter stations are exposed to more variable wind directions.

The width of the surface associated with each station is determined from the landscape unit map (ALCÁNTARA-CARRIÓ *et al.*, 1996). These values and the average density of the sediments in each station have been used to calculate the total aeolian sand transport (Table 9) from previously derived net transport values.

Aeolian sand transport pathways have been identified us-

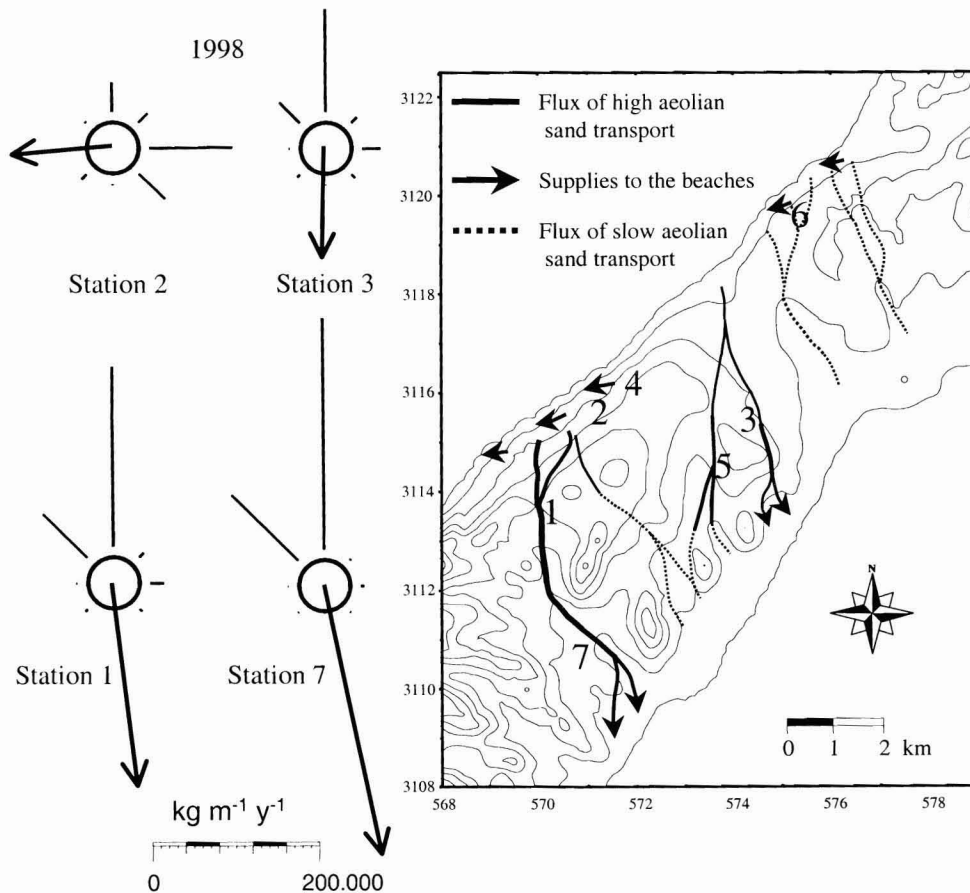


Figure 9. Annual sand roses for stations 1, 2, 3 and 7 and aeolian sand transport pathways, modified from ALCÁNTARA-CARRIÓ *et al.* (1996) and ALCÁNTARA-CARRIÓ (1999).

Table 8. Prediction of the aeolian sand transport during the whole 1998 for the four stations of Jandía Isthmus.

	Net Transport ($\text{kgm}^{-1} \text{y}^{-1}$)	Transport Direction	Wind Regimen
Station 1	247,507	173° 15' S-SSE	unimodal
Station 2	121,850	265° 45' W	bimodal
Station 3	134,237	181° 39' S	bimodal
Station 7	332,742	168° 14' S-SSE	unimodal

ing station locations and their net sediment fluxes (Figure 9). Flux across station 2 supplies equal amounts of sediment to both the windward coast and to station 1 located at the head of Wadi Pecenescal. Sediments travel from station 1 along the eastern hillside of Wadi Pecenescal to station 7, and continue on to the falling dunes and the leeward beaches. Sediments at station 3 come from the northern area of the isthmus that is covered by mobile sands, as well as from erosion associated with uncontrolled sand mining just north of this station (ALCÁNTARA-CARRIÓ *et al.*, 1996). These sediments are also transported to the leeward beaches.

The annual volume of transported sediments is large in areas around stations 1 and 2. Sediment transport at station 1 is clearly related to the trade wind direction, while the influence of the slope is crucial for station 2. The flux difference between stations 1 and 7 shows an actual accumulation of sediments in Wadi Pecenescal, which would be associated with an increase of vegetation cover as well as the influence of the sand mining between these stations, which acts to trap sediments. A reduction in the supply of sediments to the falling dunes of the leeward coast has been detected by HÖLLER-MANN (1990) and seems to continue in the present day. Sediments also reach the leeward beaches from the zone characterised by station 3. The dominant southerly littoral drift (COPEIRO, 1995) and the human occupation of the northern sector of this coastline make the flux from station 3 more important for supplying materials to the wide tidal flat and beaches of the lee coast of the Isthmus (MONTESDEOCA *et al.*, 2000). The sedimentary dynamics of the Jandía Isthmus are therefore different from those of a typical coastal isthmus in that Jandía is undergoing net erosion without present-day resupply from the windward beaches (ALCÁNTARA-CARRIÓ *et al.*, 2000a, 2000b).

CONCLUSIONS

Several of the most commonly used formulae in the literature for the prediction of aeolian sediment transport have been tested in different aeolian environments of the Jandía Isthmus by empirical transport rates obtained by vertical sand traps and simultaneous wind studies with an anemometer tower. Surface sediments and environmental factors have also been characterised. The first conclusion is that the formula for *threshold shear stress* (BAGNOLD, 1941) does not consider environmental factors. Therefore, an empirical method to determine *threshold shear stress* has been proposed, using a threshold rate of $0.01 \text{ kgm}^{-1} \text{h}^{-1}$. Predicted short-term rates using the model of ZINGG (1953) produce the best agreement with empirical rates, and its coefficient Z has

Table 9. Mass and volume of the annual aeolian sand transport at stations 1, 2, 3 and 7.

1998	Width of the Unit (m)	Density of the Sediments (kgm^{-3})	Annual Aeolian Sand Transport	
			Mass (tmy^{-1})	Volume ($\text{m}^3 \text{y}^{-1}$)
Flux 1	300	2,749.5	74,250	27,005
Flux 2	500	2,759.7	60,925	22,077
Flux 3	100	2,737.3	13,423	4,871
Flux 7	60	2,730.8	20,000	7,257

been re-calibrated. Furthermore, a new equation has been defined (VI) to calculate aeolian sediment transport. It produces predictions very similar to those of the ZINGG (1953) model and is an intermediate expression of the BAGNOLD (1941), KAWAMURA (1953) and LETTAU and LETTAU (1978) equations. Empirical average values of $Z = 1.86$ and $F = 1.97$ were found for stations with medium sand, which are in agreement with the coefficient $C = 1.8$ of BAGNOLD (1941) for medium-size, naturally-graded sand found on sand dunes.

Wind velocity profiles and local hourly wind data permit calculation of hourly wind velocity at a height of 1 m for each station during 1998. These data have been combined with other wind and sediment parameters in the calibrated equation (VI) to predict long-term aeolian sand transport at stations without the influence of a topographic slope (stations 1, 3 and 7). By contrast, the model of HARDISTY and WHITEHOUSE (1988) is chosen for station 2, with a calibration coefficient of 0.82 that is considered to be a consequence of the roughness and cohesion differences between its surface and a typical dune.

Annual transport rates at stations 7 and 1 represent the largest fluxes at Jandía isthms. However, when the surface width associated with each station is considered, most of the materials blow across the areas of stations 1 and 2. Sand transport directions are mainly to the S due to the dominance of the trade winds during the late spring and summer, which are more uniform in both velocity and direction. However, topographic slope is crucial on the windward side of the isthmus. Depositional areas for sediments eroded (blown) from the isthmus surface are 1) the falling dunes and leeward beaches and 2) the cliffs and beaches of the windward coast. At present the various aeolian environments of Jandía Isthmus are not being replenished with materials from marine sources and thus serve as the main, and potentially diminishing, sand source for the local beaches.

ACKNOWLEDGMENTS

We acknowledge with gratitude to the workers of the Aeolian Park of Cañada del Río for their help and data, as well as Teresa Baena and all the collaborators during the fieldwork. We also thank Francisco Rivero for his suggestions. This work has been funded by the Consejería de Educación, Cultura y Deportes of the Canarian Government, under research project 1/95. It is also the work number 226 of the EX1 group of the University of Vigo, contribution to projects BTE2000-0877 and IGCP-437. We thank N. Mountney and D. Jackson for their comments that helped to improve the manuscript.

LITERATURE CITED

- ALCÁNTARA-CARRIÓ, J., 1999. Dinámica sedimentaria eólica en el Istmo de Jandía. Modelización y cuantificación del transporte. Unpublished Ph.D. thesis., University of Las Palmas de Gran Canaria, Ed. Cabildo Insular de Gran Canaria, Las Palmas de Gran Canaria. 330 pp. (in Spanish).
- ALCÁNTARA-CARRIÓ, J. and ALONSO, I., 2000. Propuestas metodológicas para el estudio de los ambientes eólicos costeros. In: ANDRÉS, J.R. and GRACIA, F.J., (eds.), *Geomorfología Litoral. Procesos Activos*. Instituto Tecnológico Geominero de España. Madrid. 81–92. (in Spanish).
- ALCÁNTARA-CARRIÓ, J. and ALONSO, I., 2001. Aeolian sediment availability in coastal areas defined from sedimentary parameters. *Scientia Marina*, 65(1), 7–20.
- ALCÁNTARA-CARRIÓ, J.; ALONSO, I.; HERNÁNDEZ, L.; PÉREZ-CHACÓN, E., and ROMERO, L.E., 1996. Landscape evolution and human alterations of the aeolian dynamics in the Jandía Isthmus (Fuerteventura, Spain). In: TAUSSIK, J. and MITCHELL, J., (eds.), *Partnership in Coastal Zone Management*. Samara Publishing Ltd. Cardigan. 283–290.
- ALCÁNTARA-CARRIÓ, J.; DIZ, P.; ALEJO, I.; FRANCÉS, G.; ALONSO, I., and VILAS, F., 2000a. Contenido en foraminíferos de los depósitos eólicos del Istmo de Jandía (Fuerteventura). *Geogaceta*, 27, 195–198. (in Spanish).
- ALCÁNTARA-CARRIÓ, J.; FERNÁNDEZ-BASTERO, S.; ALEJO, I.; ALONSO, I., and VILAS, F., 2000b. Caracterización mineralógica e identificación de las áreas fuente de los sedimentos eólicos actuales del Istmo de Jandía (Fuerteventura). *Geogaceta*, 27, 199–202. (in Spanish).
- ANDERSON, R.S.; SORENSEN, M., and WILLETTS, B.B., 1991. A review of recent progress in our understanding of aeolian sediment transport. In: BARNDORFF-NIELSEN, O.E. and WILLETTS, B.B., (eds.), *Aeolian Grain Transport I, Mechanics*. Acta Mechanica Suppl. 1, 1–19.
- BAGNOLD, R.A., 1941. *The Physics of Blown Sand and Desert Dunes*. London: Methuen, 265p.
- BAGNOLD, R.A., 1956. Flow of cohesionless grains in fluids. *Philosophical Transactions Royal Society of London*, series A, 249, 235–297.
- BAUER, B.O.; DAVIDSON-ARNOTT, G.D.; NORDSTROM, K.F.; OLLERHEAD, J., and JACKSON, N.L., 1996. Indeterminacy in aeolian sediment transport across beaches. *Journal of Coastal Research*, 12(3), 641–653.
- BUER, B.O.; SHERMAN, D.J., and WOLCOTT, J.J., 1992. Sources of uncertainty in shear stress and roughness length estimates derived from velocity profiles. *Professional Geographer*, 44(4), 453–464.
- BESLER, H., 1983. The response diagram: distinction between aeolian mobility and stability of sands and aeolian residuals by grain size parameters. *Zeitschrift für Geomorphologie N. F. Supp.*, 45, 287–301.
- BRESSOLIER, C.F. and THOMAS, Y., 1977. Studies on wind and plant interactions on French Atlantic coastal dunes. *Journal of Sedimentary Petrology*, 47, 331–338.
- BURKINSHAW, J.R.; ILLEMBERGER, W.K., and CRUST, I.C., 1993. Wind-speed profiles over a reversing transverse dune. In: PYE, K. (ed.), *The Dynamics and Environmental Context of Aeolian Sedimentary Systems*. Geological Society Special Publication 72, 25–36.
- CARRACEDO, J.C.; DAY, S.J.; GUILLLOU, H.; RODRIGUEZ-BADIOLA, E.; CANAS, J.A., and PÉREZ-TORRADO, F.J., 1998. Origen y evolución del volcanismo de las Islas Canarias. In: BELMONTE AVILÉS, J. A. and SÁNCHEZ NAVARRO, J., (eds.), *Ciencia y Cultura en Canarias*. Museo de la Ciencia y el Cosmos. Tenerife. 67–89 (in Spanish).
- CHEPIL, W. S., 1945. Dynamics of wind erosion, 3. The transport capacity of the wind. *Soil Science*, 60, 475–480.
- CLEMMENSEN, L.B., 1993. *Short Course Notes*. Copenhagen, Denmark: Geologisk Institut, Kobenhavns Universitet. 48 pp.
- COELLO, J.; CANTAGREL, J.M.; HERNAN, F.; FÜSTER, J.M.; IBARROLA, E.; ANCOHEA, E.; CASQUET, C.; JAMOND, C.; DIAZ DE TERÁN, J.R., and CENDRERO, A., 1992. Evolution of the Eastern volcanic ridge of the Canary Islands based on new K-Ar data. *Journal of Volcanology and Geothermal Research*, 53, 251–274.
- COPEIRO, E., 1995. *Gestión sedimentaria del litoral canario*. Dirección Gral. de Urbanismo del Gobierno de Canarias. 97 pp. (in Spanish).
- CRIBADO, C., 1987. Evolución geomorfológica y dinámica actual del jable de Corralejo (Fuerteventura, Islas Canarias). *Revista de Geografía Canaria*, 2, 29–52. (in Spanish).
- CRIBADO, C., 1991. *La evolución del relieve de Fuerteventura*. Servicio de publicaciones del Excmo. Cabildo Insular de Fuerteventura, 318 pp. (in Spanish).
- FOLK, R.L. and WARD, W.C., 1957. Brazos river bar. A study in the significance of grain size parameters. *Journal of Sedimentary Petrology*, 27, 3–26.
- FRENZEN, P. and VOGEL, C.A., 1995. On the magnitude and apparent range of variation of the von Karman constant in the atmospheric surface layer. *Boundary-Layer Meteorology*, 72, 371–392.
- FRIEDMAN, G.M. and SANDERS, J.E., 1978. *Principles of Sedimentology*. New York: Wiley, 792 pp.
- FRYBERGER, S.G. and DEAN, G., 1979. Dune forms and wind regimen. In: MCKEE, E.D., (ed.), *A Study of Global Sand Seas*. Washington, DC: U. S. Geol. Survey Prof. Paper 1052. pp. 137–169.
- GLÄSER, B., 1984. Quantitative untersuchungen zur morphogenese und mobilität des Alt-dünenkomplexes in der Provinz Weiber Nil. In: MENSCHING, H., (ed.), *Beiträge zur morphodynamik im Relief des Jebel-Marra-Massivs und in seinem Vorland (Darfur / Republik Sudan)*. Akad. d. Wissensch. Göttingen, Hamburg. 202–217. (in German)
- HARDISTY, J. and WHITEHOUSE, R.J.S., 1988. Evidence for a new sand transport process from experiments on Sahara dunes. *Nature*, 332, 532–534.
- HÖLLERMANN, P., 1990. Zur Geoökodynamik von Dünen; eine Fallstudie aus Süd; Fuerteventura (Kanarische Inseln). *Geoökodynamik*, 11, 213–240.
- HORIKAWA, K.; HOTTA, S., and KRAUS, N., 1986. Literature review of sand transport by wind on a dry sand surface. *Coastal Engineering*, 9, 503–526.
- HSU, S.A., 1973. Computing eolian sand transport from shear velocity measurements. *Journal of Geology*, 81, 739–743.
- HSU, S.A., 1977. Boundary layer meteorological research in the coastal zone. *Geoscience and Man*, 18, 99–111.
- ILLEMBERGER, W.K. and RUST, I.C., 1986. Venturi-compensated eolian sand trap for field use. *Journal of Sedimentary Petrology*, 56(4), 541–543.
- KAWAMURA, R., 1951. *Study on blown sand by wind*. Translated as Technical report Hydraulic Engineering Laboratory. University of California, Berkeley. 57 pp.
- LANCASTER, N. and BAAS, A., 1998. Influence of vegetation cover on sand transport by wind: field studies at Owens Lake, California. *Earth Surface Processes and Landforms*, 23, 69–82.
- LARSON, M. and KRAUS, N.C., 1995. Prediction of cross-shore sediment transport at different spatial and temporal scales. *Marine Geology*, 126, 111–127.
- LEATHERMAN, S.P., 1978. A new aeolian sand trap design. *Sedimentology*, 25, 303–306.
- LE BAS, M.J.; REX, D.C., and STILLMAN, C.J., 1986. The early magmatic chronology of Fuerteventura, Canary Islands, *Geological Magazine*, 123(3), 287–298.
- LETTAU, K. and LETTAU, H., 1978. Experimental and micrometeorological field studies of dune migration. In: LETTAU, K. and LETTAU, H., (eds.), *Exploring the world's driest climate*. University of Wisconsin-Madison, IES Report 101, 110–147.
- LOGIE, M., 1982. Influence of roughness elements and soil moisture of sand to wind erosion. *Catena Supplement*, 1, 161–173.
- MCDONALD, G.A.; ABBOT, A.T., and PETERSON, F.L., 1970. *Volcanoes in the Sea*. Honolulu: University of Hawaii Press. 517p.
- MCEWAN, I.K. and WILLETTS, B.B., 1993. Sand transport by wind: a review of the current conceptual model. In: PYE, K., (ed.), *The dynamics and environmental context of aeolian sedimentary systems*. Geological Society Special Publication, 72, 7–16.
- MECO, J., 1993. Testimonios paleoclimáticos en Fuerteventura. *Tierra y Tecnología*, 6, 41–48. (in Spanish).
- MILLER, M.; MCCAVE, I.N., and KOMAR, P.D., 1977. Threshold of sediment motion under unidirectional currents. *Sedimentology*, 24, 504–527.
- MONTESDEOCA, I.; ALONSO, I.; ALCÁNTARA-CARRIÓ, J.; CABRERA, L., and VIVARES, A., 2000. Dinámica sedimentaria en la Playa de la Barca

(Jandía, Fuerteventura). Variabilidad morfológica y granulométrica. *Geotemas*, 1(4), 191–194.

NICKLING, W.G. and ECCLESTONE, M., 1981. The effects of soluble salts on the threshold shear velocity of fine sand. *Sedimentology*, 31, 111–117.

NORDSTROM, K.F., 1994. Beaches and dunes of human altered coasts. *Progress in Physical Geography*, 18 (4), 497–516.

OWEN, P.R., 1964. Saltation of uniform grains in air. *Journal of Fluid Mechanics*, 20 (2), 225–242.

SARRE, R.D., 1987. Aeolian sand transport. *Progress in Physical Geography*, 11, 155–182.

SEELIGER, U.; CORDAZZO, C.V.; OLIVEIRA, C.P.L., and SEELIGER, M., 2000. Long-term changes of foredunes in the Southwest Atlantic. *Journal of Coastal Research*, 16 (4), 1068–1072.

SHERMAN, D.J. and HOTTA, S., 1990. Aeolian sediment transport: theory and measurements. In: NORDSTROM, K.F.; PSUTY, N., and CARTER, B., (eds.), *Coastal Dunes, Form and Process*. Chichester: Wiley, pp. 17–37.

SHORT, A.D. and HESP, P., 1982. Wave, beach and dune interactions in southeastern Australia. *Marine Geology*, 48, 259–284.

TSOAR H. and PYE, K., 1987. Dust transport and the question of desert loess formation. *Sedimentology*, 34, 139–153.

VON KARMAN, T., 1934. Turbulence and skin friction. *Journal of Aeronautical Science*, 1, 1–20.

WILLIAMS, G., 1964. Some aspects of the eolian saltation load. *Sedimentology*, 3, 257–287.

ZINGG, A.W., 1953. Wind tunnel studies of the movement of sedimentary material. *Proceedings of the 5th Hydraulics Conference Bulletin* Institute of Hydraulics of Iowa City, 34, 111–135.

APPENDIX I.

Table I.1. Monthly ($kgm^{-1} month^{-1}$) and annual ($kgm^{-1} year^{-1}$) transport rates predicted for station 1.

Station 1	Predicted Rates of Aeolian Sediment Transport From Each Direction								
	1998	N	NE	E	SE	S	SW	W	NW
January	4,867	372	65	652	129	797	321	199	
February	20	939	6,293	2,564	0	2,731	59	51	
March	13,474	4,405	1,816	135	58	0	32	695	
April	33,836	0	0	0	0	0	0	1,385	
May	8,835	0	0	0	16	0	4	676	
June	24,059	0	0	0	0	0	48	10,255	
July	46,969	35	0	0	0	0	117	31,722	
August	37,841	0	0	0	0	0	0	18,464	
September	9,574	0	0	0	0	0	0	2,923	
October	14,542	417	1,077	0	0	0	0	802	
November	3,696	307	1,210	0	0	0	0	51	
December	816	174	4,318	672	0	6	206	807	
Annual	198,533	6,651	14,781	4,025	204	3,535	791	68,035	

Table I.3. Monthly ($kgm^{-1} month^{-1}$) and annual ($kgm^{-1} year^{-1}$) transport rates predicted for station 2.

Station 2	Predicted Rates of Aeolian Sediment Transport From Each Direction								
	1998	N	NE	E	SE	S	SW	W	NW
January	4,203	783	397	6,370	769	1,697	266	114	
February	16	1,983	38,592	25,322	6	5,920	499	29	
March	11,745	9,602	11,098	1,317	346	0	26	400	
April	30	0	0	0	0	0	0	0	
May	0	0	0	0	0	0	0	0	
June	15	0	0	0	0	0	0	7	
July	69	0	0	0	0	0	0	39	
August	38	0	0	0	0	0	0	12	
September	1	0	0	0	0	0	0	0	
October	12,558	874	6,545	0	0	0	0	461	
November	3,131	651	7,331	11	0	0	0	29	
December	681	361	26,340	6,794	0	13	171	480	
Annual	32,491	14,257	90,304	39,815	1,121	7,631	513	1,575	

Table I.2. Sand transport parameters for station 1.

Station 1	RDP	RDD	DP	RDP/DP	Classification
January	4,124	176° 42'	7,404	0.56	bimodal
February	7,390	294° 09'	12,661	0.58	bimodal
March	17,516	194° 53'	20,617	0.85	unimodal
April	34,829	178° 23'	35,222	0.99	unimodal
May	9,309	177° 01'	9,532	0.98	unimodal
June	32,150	166° 52'	34,362	0.94	unimodal
July	72,988	162° 01'	78,845	0.93	unimodal
August	52,545	165° 36'	56,305	0.93	unimodal
September	11,824	169° 55'	12,498	0.95	unimodal
October	15,425	182° 59'	16,839	0.92	unimodal
November	4,187	199° 25'	5,266	0.80	unimodal
December	4,261	256° 00'	7,002	0.61	bimodal
Annual	247,507	173° 15'	296,558	0.83	unimodal

Table I.4. Sand transport parameters for station 2.

Station 2	RDP	RDD	DP	RDP/DP	Classification
January	5,215	292° 42'	14,604	0.36	bimodal
February	57,484	291° 01'	71,919	0.80	unimodal
March	25,501	266° 35'	34,536	0.74	bimodal
April	30	179° 59'	30	1.00	unimodal
May	0	180° 00'	0	1.00	unimodal
June	21	166° 02'	22	0.93	unimodal
July	101	163° 53'	109	0.93	unimodal
August	47	169° 30'	50	0.94	unimodal
September	1	178° 17'	1	0.99	unimodal
October	15,135	206° 51'	20,439	0.74	bimodal
November	8,573	245° 08'	11,154	0.77	bimodal
December	31,081	276° 32'	34,842	0.89	unimodal
Annual	121,850	265° 45'	187,712	0.65	bimodal

Table I.5. Monthly ($kg\ m^{-1}\ month^{-1}$) and annual ($kg\ m^{-1}\ year^{-1}$) transport rates predicted for station 3.

Station 3 1998	Predicted Rates of Aeolian Sediment Transport From Each Direction							
	N	NE	E	SE	S	SW	W	NW
January	6,248	605	194	1,008	231	1,096	514	361
February	65	1,350	8,268	3,554	6	3,376	108	148
March	15,883	5,275	2,548	315	134	0	83	1,255
April	13,985	11	5	0	0	1	14	779
May	4,851	3	0	11	27	0	9	596
June	10,137	0	0	5	0	0	30	4,559
July	17,774	20	0	0	0	2	62	12,057
August	15,047	0	0	0	0	0	3	7,533
September	4,656	15	18	0	0	0	0	1,645
October	18,153	637	1,542	1	0	0	0	1,442
November	5,128	483	1,739	11	0	0	0	135
December	1,297	385	6,041	812	0	22	349	1,110
Annual	113,230	8,789	20,360	5,720	400	4,499	1,176	31,626

Table I.6. Sand transport parameters for station 3.

Station 3	RDP	RDD	DP	RDP/DP	Classification
January	1,003	177° 41'	10,259	0.10	complex
February	9,887	292° 29'	16,880	0.59	bimodal
March	20,889	195° 21'	25,496	0.82	unimodal
April	14,554	177° 49'	14,798	0.98	unimodal
May	5,257	175° 24'	5,501	0.96	unimodal
June	13,748	166° 19'	14,733	0.93	unimodal
July	27,675	161° 56'	29,917	0.93	unimodal
August	21,060	165° 20'	22,584	0.93	unimodal
September	5,940	168° 59'	6,336	0.94	unimodal
October	19,646	182° 50'	21,777	0.90	unimodal
November	5,905	199° 43'	7,498	0.79	bimodal
December	6,003	252° 53'	10,018	0.60	bimodal
Annual	134,237	181° 39'	185,803	0.72	bimodal

Table I.7. Monthly ($kg\ m^{-1}\ month^{-1}$) and annual ($kg\ m^{-1}\ year^{-1}$) transport rates predicted for station 7.

Station 7 1998	Predicted Rates of Aeolian Sediment Transport From Each Direction							
	N	NE	E	SE	S	SW	W	NW
January	1,193	97	17	172	35	203	86	56
February	5	244	1,567	653	0	663	16	14
March	3,214	1,054	459	38	16	0	8	191
April	51,590	24	1	0	0	0	42	3,421
May	20,587	0	0	0	158	5	36	3,239
June	37,603	0	0	0	0	0	109	17,561
July	62,125	86	0	0	0	0	250	42,509
August	54,149	0	0	0	0	0	13	27,594
September	18,653	22	0	0	0	0	0	7,117
October	3,555	111	275	0	0	0	0	221
November	946	79	312	0	0	0	0	14
December	218	49	1,096	160	0	1	56	205
Annual	253,842	1,769	3,730	1,024	210	874	620	102,148

Table I.8. Sand transport parameters for station 7.

Station 7	RDP	RDD	DP	RDP/DP	Classification
January	1,003	176° 27'	1,862	0.54	bimodal
February	1,860	293° 32'	3,165	0.59	bimodal
March	4,195	195° 01'	4,984	0.84	unimodal
April	54,081	177° 24'	55,079	0.98	unimodal
May	22,835	174° 08'	24,026	0.95	unimodal
June	51,565	165° 56'	55,274	0.93	unimodal
July	97,078	161° 50'	104,972	0.92	unimodal
August	76,205	165° 09'	81,757	0.93	unimodal
September	24,226	168° 02'	25,792	0.94	unimodal
October	3,795	182° 58'	4,163	0.91	unimodal
November	1,074	199° 28'	1,353	0.79	bimodal
December	1,079	254° 48'	1,787	0.60	bimodal
Annual	332,742	168° 14'	364,220	0.91	unimodal